

RESEARCH ARTICLE

Adaptive Grid Partitioning Considering Power Supply and Load Distribution

GANG YAO, YOUQIAN ZHANG, TAO ZHANG, QINFENG MA^{ID}, AND JINLONG CHEN

Power Dispatch Control Center of Guizhou Power Grid Company Ltd., Guiyang 550002, China

Corresponding author: Gang Yao (2565752184@qq.com)

This work was supported by the Key Science and Technology Project of China Southern Power Grid Company Ltd., under Grant GZKJXM20210372.

ABSTRACT Renewable energy such as wind power, hydro-power and photovoltaic are connected to the power system as distributed power sources will increase the instability of power system operation. To ensure the stable operation of the power system after renewable energy and load access, it is necessary to properly partition the power grid. A grid partition method considering renewable energy access and load fluctuation is proposed. First, cluster analysis was carried out on the operation scenarios of renewable energy and load by using the improved K-means algorithm, and several operation scenarios of power system were obtained. The three operation scenarios with the highest probability were selected as the three normal operation states of power system. Then, the power system is partitioned, and the comprehensive flexibility evaluation indexes are proposed from the perspectives of regional supply and demand balance and inter-regional transmission capacity. The flexibility evaluation indexes from these two perspectives are calculated under three operating states, and the two flexibility evaluation indexes are weighted to evaluate the comprehensive flexibility of the power system after the partition. The comprehensive flexibility index of the power system is different under different partition strategies. The partition strategy with the best evaluation of the comprehensive flexibility index is chosen as the final partition strategy. Finally, according to the historical data of renewable energy and load in a certain region, the IEEE 39-bus system with renewable energy access and load fluctuation is partitioned under different partitioning strategies, and the comprehensive flexibility of the partitioned power system is evaluated, and the final partitioning strategy is determined according to the comprehensive flexibility index of the power system.

INDEX TERMS Adaptive partition, renewable energy, power system, flexibility evaluation index.

I. INTRODUCTION

In recent years, China's renewable new energy has been developing rapidly. Installed capacity of hydro-power units has been increasing every year, and both wind power and photovoltaic units rank first in the world. But at the same time, with the access of wind power, hydro-power, photovoltaic and other renewable new energy, because of their intermittence and load fluctuation, bring great instability to the operation of the power system [1], [2]. Renewable energy generation will be the distributed power source in the future power grid and will be widely used in the future. Therefore, the influence of these distributed power sources on the stable operation of

the power system should be fully considered [3], [4], [5]. Network reconfiguration is performed by reconfiguring the power network. System reconfiguration means restructuring the power lines which connect various buses in a power system. Restructuring of specific lines leads to alternate system configurations. It's difference with grid partitioning, it does not need to divide the power system into multiple zones. System reconfiguration can be accomplished by placing line interconnection switches into network [6]. Both network reconfiguration and grid partitioning can solve the problem of supply and demand balance caused by distributed power resources and load. This paper completes the redistribution of distributed power resources and load through grid partitioning. At present, the wind abandoning and light abandoning rates are relatively high in some parts of China's power

The associate editor coordinating the review of this manuscript and approving it for publication was Ton Duc Do^{ID}.

system, and the flexibility of some parts for high proportion of renewable energy access is far from enough. This has a great impact on the balance of supply and demand within the power system partition and the power transmission between the partitions, resulting in the normal operation of the power system [7], [8], [9]. Therefore, the flexibility of the power system should be fully considered in the planning zoning of the power grid, and the results of the planning zoning should ensure that the flexibility index requirements are met, so that the uncertainty of renewable energy and load fluctuation in each region can be effectively matched, to ensure the stable operation of the power system after the zoning.

To consider flexibility indicators in the zoning planning stage, it is necessary to accurately evaluate the overall and regional flexibility of the power system after zoning. But at present the definition of power system flexibility index has not been determined. The International Energy Agency defines the power system flexibility as the response speed and anti-interference ability of the power system in the face of predicted fluctuations and disturbances outside the forecast [10]. According to the North American Power Reliability Association, system flexibility is the ability to respond to uncertainties in the system by mobilizing resources at your disposal. The [11] evaluates power system flexibility from a net load demand perspective. The [8] evaluated the flexibility of the power system by using power climbing rate as an indicator. The [12] took the period of insufficient flexibility resources and the expectation of insufficient climbing resources as the evaluation indexes of flexibility.

The above studies mainly evaluate the power system from the perspective of flexible supply and demand. However, in the evaluation, the good flexibility of the power system is not only reflected in meeting the balance of supply and demand within the region, but also needs to meet the requirements of inter-regional power transmission. For example, there is a large flexible supply and demand in a certain region, but the electric energy transmission between this region and other regions may not meet the requirements of electric energy transmission [13], [14], [15], [16]. As a result, the line load rate of the entire power system is too high, and the transmission channel cannot carry the transmitted electric energy, making the power system unable to operate safely and stably [17]. Therefore, when analyzing the flexibility of the power system, it is necessary to consider both the supply and demand within the region and the flexibility of the transmission channel between regions [18], [19]. Only when both meet the requirements can the safe and stable operation of the power system be guaranteed.

In this paper, a grid partitioning method based on intra-regional supply and demand balance flexibility and inter-regional transmission flexibility is proposed. In section II, cluster analysis was carried out on the operation scenarios of renewable energy and load by using the improved K-means algorithm, and several operation scenarios of power system were obtained. The three operation scenarios with the highest probability were selected as the three normal

operation states of power system. In section III, the flexibility index of supply and demand balance and the flexibility index of inter-regional transmission are proposed, and the comprehensive flexibility evaluation indexes are proposed from the two perspectives. The comprehensive flexibility index of the power system is different under different partition strategies. The partition strategy with the best evaluation of the comprehensive flexibility index is chosen as the final partition strategy. In section IV, according to the historical data of renewable energy and load in a certain region, the IEEE 39-bus system with renewable energy access and load fluctuation is partitioned under different partitioning strategies, and the comprehensive flexibility of the partitioned power system is evaluated, and the final partitioning strategy is determined according to the comprehensive flexibility index of the power system.

II. OPERATING SCENARIO GENERATION

A. IMPROVE K-MEANS CLUSTERING ALGORITHM

K-means clustering algorithm is widely used because of its simplicity and high efficiency. The k-means algorithm is a classic clustering algorithm. Generally, Euclidean distance is used as an evaluation index of the similarity of two samples. The basic idea is as follows: the data are divided into K groups in advance, then K objects are randomly selected as the initial cluster center. Then the distance between each object and each cluster center is calculated and each object is assigned to the cluster center closest to it. The cluster centers and the objects assigned to them represent a cluster. For each sample assigned, the clustering center of the cluster is recalculated based on the existing objects in the cluster. This process is repeated until a certain termination condition is met. The termination condition may be that no objects are reassigned to different clusters, no cluster centers change again and the squared error and local minimum. The flowchart of k-means algorithm is shown in Figure 1. The pseudo code of k-means algorithm is shown in Figure 2.

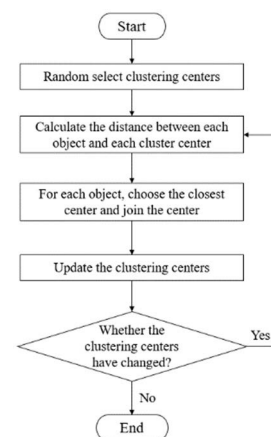


FIGURE 1. Flowchart of k-means algorithm.

However, the general K-means clustering algorithm needs to determine the number of clustering centers first, and the

```

#k-means pseudo code
import numpy as np
import copy
#Calculate the Euclidean distance
def get_distance(X,Y):
    return np.sum((X-Y)**2)**0.5
def calc_mean(X): # Calculate the center point and take the mean of each dimension
    l=len(X[0])
    list_mean= [ ]
    for i in range(l):
        s=0
        for j in X:
            s+=j[i]
        m=s/len(X)
        list_mean.append(m)
    return list_mean
def k_means(x_train,max_iter):
    num_iter = 0
    # Initial cluster center
    cluster_center = x_train[k]
    pre_cluster_center = copy.deepcopy(cluster_center) # The center of the cluster last time
    # Start the iteration
    while num_iter<max_iter:
        # Temporary variable
        clusters_data= { } # Dictionary {cluster subscript: coordinates}
        for i in x_train:
            cluster_dists= [ ]
            for index,cluster in enumerate(cluster_center):
                distance=get_distance(i,cluster)
                cluster_dists.append((index,distance)) # The distance from the center of each
            cluster_dists.sort(key=lambda x:x[1]) # Ascending
            min_index,min_dist=cluster_dists[0] # Take the closest distance
            if min_index not in clusters_data:
                clusters_data[min_index]= [ ]
                clusters_data[min_index].append(i) # Data is added to a temporary variable
        # Update cluster center point
        for index in clusters_data:
            cluster_center[index]=calc_mean(clusters_data[index])
        if pre_cluster_center == cluster_center:
            break # If the cluster center does not change, then end
        else:
            pre_cluster_center = copy.deepcopy(cluster_center) #Copy
    return cluster_center # Returns the final cluster center point

```

FIGURE 2. Pseudo code of k-means algorithm.

specific number is unknown in most cases. However, if the number of clustering centers is not set properly, the final clustering result will have a large error [20], [21], [22]. Therefore, Canopy algorithm was used to improve the K-means clustering algorithm, and the improved K-means clustering algorithm was used to perform cluster analysis on the existing renewable energy and load data. Before clustering, Canopy algorithm was used for a rough clustering of existing data to determine the number of clustering centers. Canopy algorithm does not need to set the number of clusters in advance like the general K-means algorithm and can perform rough clustering of data in the data pre-processing stage. Then, according to the results of rough clustering, k-means algorithm is used to cluster the data, to optimize the clustering results. The specific steps of Canopy algorithm are as follows [23], [24]:

Step 1: Input the set L composed of original data, set the distance threshold S_1 and S_2 , and $S_1 > S_2$.

Step 2: Randomly select data point P from L , set point P as Canopy of the first data center, and delete it from L .

Step 3: Take a point N from L and calculate the distance between point N and the existing point P . If the distance between point N and point P is less than S_2 , add point N to point P and set it as set C . Then delete point N from L , so that

the distance between point N and P is close enough. If the distance from point N to point P is greater than S_1 , point N is treated as a new point P and removed from L . If the distance from point N to point P is between S_1 and S_2 , point N is added to set C , but not removed from L , and continues to participate in subsequent calculations.

Step 4: Repeat step 3 for other points of L until there is no data in L .

The flowchart of Canopy algorithm is as Figure 3.

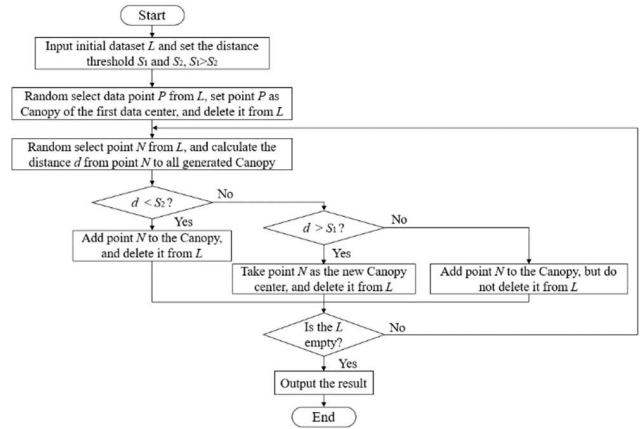


FIGURE 3. Flowchart of the canopy algorithm.

The result of the number of rough clustering obtained by Canopy algorithm was taken as the number of clustering centers of k-means clustering, and the final clustering result was obtained.

B. SCENARIO OF POWER SYSTEM OPERATION

In the electric power system, with the access of large amounts of renewable energy and load, the uncertainty of renewable energy and the fluctuation of load will increase the instability of the operation of the power system, resulting in the irregular output data and load data of new energy sources in a year. Therefore, it is necessary to cluster the output data and load data of renewable energy power sources in a year to obtain the various operation scenarios. However, if the improved clustering analysis is carried out for each unit and load data, the number of each cluster may be different, increasing the complexity and computation of subsequent analysis. Therefore, it is necessary to define the operation scenario of power supply and load, that is, the operation scenario that takes all the renewable energy and load in the system as a whole. Each operation scenario includes output and load fluctuations for each renewable power source. In the clustering process, the optimal number of clustering centers was obtained by using Canopy algorithm for each renewable energy source and load. Then, k-means clustering is performed to obtain the operation scenarios of renewable energy power supply and load. The specific process is as follows:

First, the historical curves of n new energy power sources were analyzed by Canopy rough clustering, and the number of rough clustering centers c_i ($1 \leq i \leq n$) of output of each

power source was obtained. Take c_i , which appears most in all the coarse clustering numbers, and take this clustering center number as the optimal clustering number (c) of the operation scenario of power supply. Then, c is taken as the number of clustering centers of the next K-means clustering algorithm to conduct a unified clustering analysis on the power supply operation scenarios and obtain the power supply operation scenarios. At the same time, the occurrence probability of each scenario can be obtained according to the historical data contained in each scenario. The clustering process of load data is the same as the clustering process of power supply, which is not described here. After the clustering results of power supply (assuming c_1 scenarios) and load (assuming c_2 scenarios) are obtained, the various scenarios of power supply and load are combined in pairs to obtain $c_1 \times c_2$ operating scenarios of the system and the occurrence probability $P_a \times P_b$ ($1 \leq a \leq c_1, 1 \leq b \leq c_2$) of each operating scenario.

III. POWER SYSTEM FLEXIBILITY ASSESSMENT

A certain power system is partitioned, and flexibility assessment is carried out within and between regions of the power system respectively. The assessment indicators are shown in Figure 4.

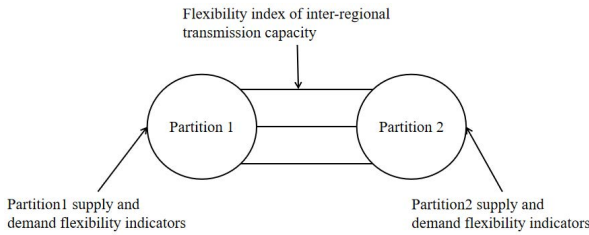


FIGURE 4. Diagram of flexibility evaluation index.

The flexibility evaluation index in the region includes the poor flexibility index on supply and demand in the region. The inter-regional flexibility assessment index includes the poor flexibility index of inter-regional transmission capacity [25].

A. REGIONAL SUPPLY AND DEMAND

The flexibility index of supply and demand is an index to determine whether flexibility of supply in the zone can meet the flexibility of demand in the zone.

The Figure 5 shows the flexibility resources diagram of the zone. In the zone, flexibility resources are divided into two parts, flexibility demand and flexibility supply. Flexibility

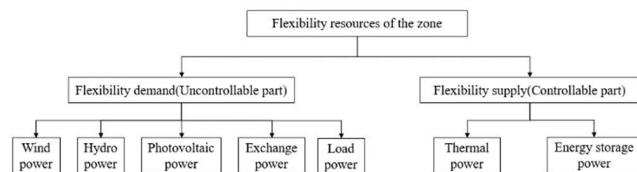


FIGURE 5. The flexibility resources diagram of the zone.

demand is generated from uncontrollable parts, such as wind power, hydro power, photovoltaic power, exchange power and load power. Flexibility supply is generated from controllable parts such as thermal power and energy storage power.

In the partition, the power demand and supply generated by uncontrollable units and loads at time t are as follows:

$$P_{un_de}(t) = P_l(t) + \Delta P(t) \quad (1)$$

$$P_{un_sup}(t) = P_w(t) + P_p(t) + P_h(t) \quad (2)$$

where $P_l(t)$, $P_w(t)$, $P_p(t)$ and $P_h(t)$ are the load output power, wind power output power, photovoltaic output power and hydro-power output power of each zone respectively; $\Delta P(t)$ is the power exchanged between the partition and the outside world. When $\Delta P(t) > 0$, it is considered that the partition transmits power to the outside and increases the power demand; When $\Delta P(t) < 0$, the partition receives power from the outside and reduces the power demand.

The upper and lower limits of the power demand change of the uncontrollable part are:

$$P_{un_de_max}(t) = (1 + \mu) P_{un_de}(t) - (1 - \mu) P_{un_sup}(t) \quad (3)$$

$$P_{un_de_min}(t) = (1 - \mu) P_{un_de}(t) - (1 + \mu) P_{un_sup}(t) \quad (4)$$

where μ is the power fluctuation coefficient. The larger μ is, the greater the power fluctuation is.

According to the variation range of power demand above, the calculation method of regional flexibility demand is as follows, as shown in Figure 2.

When $P_{un_de_min}(t) > P_{un_de}(t - 1)$, only up flexibility requirements:

$$P_{de_up}(t) = P_{un_de_max}(t) - P_{un_de}(t - 1) \quad (5)$$

When $P_{un_de_max}(t) > P_{un_de}(t - 1) > P_{un_de_min}(t)$, there are both upward flexibility requirements and downward flexibility requirements:

$$\begin{cases} P_{de_up}(t) = P_{un_de_max}(t) - P_{un_de}(t - 1) \\ P_{de_down}(t) = P_{un_de}(t - 1) - P_{un_de_min}(t) \end{cases} \quad (6)$$

When $P_{un_de}(t - 1) > P_{un_de_max}(t)$, only down flexibility requirements:

$$P_{de_down}(t) = P_{un_de}(t - 1) - P_{un_de_min}(t) \quad (7)$$

Regional upward and downward flexibility supply is provided by thermal power units and energy storage devices, and the calculation process is as follows:

$$P_{sup_up}(t) = P_{con_max} - P_{con}(t) \quad (8)$$

$$P_{sup_down}(t) = P_{con}(t) - P_{con_min} \quad (9)$$

where $P_{con}(t)$ is the output value of the controllable unit; P_{con_max} and P_{con_min} are the maximum and minimum output values of all controllable units respectively.

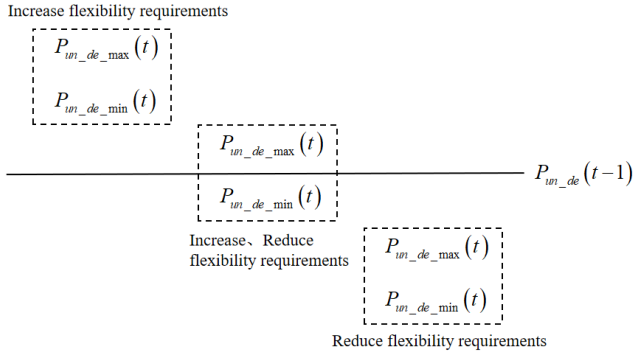


FIGURE 6. Diagram of upward and downward flexibility demand.

Based on the above mentioned upward and downward flexibility demand and supply, the index of upward and downward flexibility can be obtained [25]:

$$K_{up}(t) = \frac{P_{de_up}(t)}{P_{sup_up}(t)} \quad (10)$$

$$K_{down}(t) = \frac{P_{de_down}(t)}{P_{sup_down}(t)} \quad (11)$$

Up and down poor flexibility index indicates the ability of flexible resources to meet up and down flexibility requirements. When $K_{up}(t) < 1$, $P_{sup_up}(t) > P_{de_up}(t)$, Flexible resources meet the needs of power grid, there is a certain margin. When $K_{up}(t) > 1$, $P_{sup_up}(t) < P_{de_up}(t)$, Flexible resources may not be able to meet the needs of the power grid, so measures such as increasing the installed capacity of controllable units, energy storage, renewable energy or cutting off load should be taken to ensure the balance between supply and demand of flexible resources in the region. In the same way, when $K_{down}(t) > 1$, Flexible resources cannot meet the needs of power grid, so measures such as reducing renewable energy and increasing load should be taken to ensure the balance between supply and demand of flexible resources in the region.

B. INTER-REGIONAL TRANSMISSION CAPACITY

Since some areas have more renewable energy and less load, the power demand in these areas cannot fully absorb the electricity generated by renewable energy, and a large amount of electricity needs to be transferred to other areas. Therefore, the flexibility index of transmission capacity is defined to judge whether the transmission capacity of the inter-regional transmission channel meets the transmission power.

According to the power transmission direction relationship between regions, the two ends of the transmission channel between regions are divided into the transmitting end and the receiving end. Assume that there are n transmission lines between the transmitting end and the receiving end, define the active power of each line as P_i ($i = 1, 2, \dots, n$), the transmission channel constituted by it is shown in Figure 7.

For the transmitting end, its transmitting power at time t is:

$$P_{sup}(t) = P_w(t) + P_p(t) + P_h(t) + P_{con}(t) - P_l(t) - \Delta P(t) \quad (12)$$

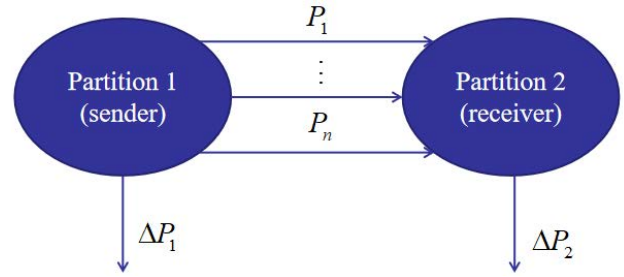


FIGURE 7. Diagram of a transmission channel.

Regardless of the line transmission loss between regions, the transmitted power at the sending end is the transmitted power of the transmission channel between regions:

$$P_{sup}(t) = P_{tra}(t) = P_1(t) + P_2(t) + \dots + P_n(t) \quad (13)$$

Power distribution coefficients of line 1 ~ n in the transmission channel are defined as $\rho_1, \rho_2, \dots, \rho_n$, so there are:

$$P_{tra}(t) = P_1(t) + P_2(t) + \dots + P_n(t) = \rho_1 P_{tra}(t) + \rho_2 P_{tra}(t) + \dots + \rho_n P_{tra}(t) = \sum_{i=1}^n \rho_i P_{tra}(t) \quad (14)$$

where ρ_i is the power distribution coefficient of transmission line i , and $\sum_{i=1}^n \rho_i = 1$. For different system operation scenarios, the power distribution coefficients of transmission lines are different, but for the same system operation scenarios, it's believed that the power distribution coefficients of transmission lines are the same. ρ_i is defined as follows:

$$\rho_i = \frac{\bar{P}_i}{\sum_{i=1}^n \bar{P}_i} \quad (15)$$

where \bar{P}_i is the average power of transmission line i . \bar{P}_i is defined as follows:

$$\bar{P}_i = \frac{1}{T} \sum_{t=1}^T P_i(t) \quad (16)$$

In the transmission process, if one transmission line in the transmission channel reaches the transmission power upper limit, that is:

$$\rho_i P_{tra}(t) = P_{max} \quad (17)$$

Thus, it's thought that the total transmitted power between the sender and the receiver has reached its limit. Calculate the total transmitted power of each line when it reaches the power upper limit, and take the minimum value as the transmission power upper limit of the inter-regional transmission channel:

$$P_{sum_max} = \min_{1 < i < n} \frac{P_{max}}{\rho_i} \quad (18)$$

The maximum power sent by the sending end is defined as:

$$P_{s_max} = \max(t | P_w(t) + P_p(t) + P_h(t) + \min(t | P_{con}(t)) - \min(t | P_l(t)) - \min(\Delta P_r(t)) \quad (19)$$

where $\Delta P_r(t)$ is the power exchanged between the sender and other regions (not the receiver).

The poor flexibility index of inter-regional transmission capacity is [25]:

$$K_{cap} = \frac{P_{s_max}}{P_{sum_max}} \quad (20)$$

If $K_{cap} > 1$, this indicates that the inter-regional transmission capacity is not flexible enough. When the output power of the transmitter power reaches its maximum, the transmission capacity of the transmission channel cannot meet the transmission demand. In this case, new inter-regional transmission lines are required. If $K_{cap} = 1$, it means that the transmission capacity of the transmission channel just meets the transmission demand of the maximum output power of the transmitting end. If $K_{cap} < 1$, it shows that the transmission capacity of the transmission channel is flexible and the process of electric energy transmission will not be hindered.

C. COMPREHENSIVE EVALUATION INDEX

The regional supply-demand downward flexibility index and inter-regional transmission capacity flexibility index mentioned above only evaluate the local flexibility of the power system after zoning, but also need to evaluate the overall flexibility of the power system after zoning. The following composite poor flexibility index is:

$$K_{com} = w_1 \bar{K}_{up}(t) + w_2 \bar{K}_{down}(t) + w_3 \bar{K}_{cap} \quad (21)$$

where $\bar{K}_{up}(t)$, $\bar{K}_{down}(t)$, \bar{K}_{cap} is the average value of up, down and inter-regional transmission capacity poor flexibility index. w_1 , w_2 , w_3 is the weighting coefficient.

The comprehensive poor flexibility index reflects the stability ability of the whole power system after partitioning. The smaller the comprehensive poor flexibility index is, the better the overall flexibility of the power system is, that is, the better the partitioning effect of the power system is. The effect of power grid partitioning is evaluated by the comprehensive flexibility index. The partition result corresponding to the lowest comprehensive poor flexibility index is selected as the partition scheme.

IV. CASE STUDY

According to the output data and load data of wind power, photovoltaic power and hydro-power in a certain region, the improved IEEE39-node system is evaluated and tested for zoning and flexibility, and the overall flexibility of the system under different zoning strategies is analyzed and evaluated, to select the zoning strategy with the best overall flexibility of the system.

Take three partitions as an example, the IEEE39-bus test system is divided into three zones. As shown in Figure 8.

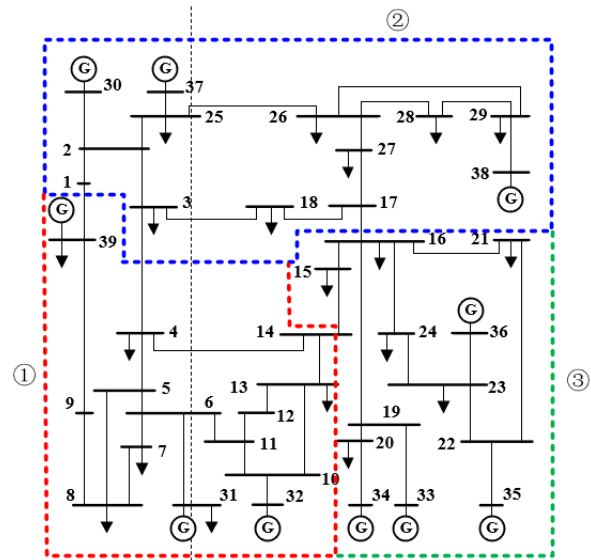


FIGURE 8. Diagram of zones.

Unit G is the power supply. The configuration of renewable energy power supply is shown in Table 1. The thermal power unit (controllable power supply) is connected to nodes 32, 34, 36, 37, and 39. The total capacity of the unit is 5000 MW, and the total capacity of the renewable energy unit is 700 MW. Access fluctuating loads at nodes 2, 6, 11, 14, 17, 19, 22, 36, 38. Except for nodes connected to renewable energy units and fluctuating loads, the power supply and loads of other nodes are fixed. The transmission channel capacity between each subdivision is 1000 MVA. Set the power fluctuation coefficient as 0.15. Then the system is divided into four, five and six partitions to find the best partitioning strategy for the overall flexibility of the system.

TABLE 1. Renewable source configuration of system.

The unit type	Node	Unit capacity
Wind power	30	200MW
Wind power	31	200MW
Photovoltaic	33	100MW
Photovoltaic	35	100MW
Hydro-power	38	100MW

A. TYPICAL SCENARIO

The annual historical data of renewable energy and fluctuating load were used as the basic data for clustering and scene division, and the 24-hour data of typical scenarios were obtained.

First, Canopy algorithm was used to perform rough clustering for the annual historical data of each renewable energy source and fluctuating load to obtain the optimal clustering number. According to the results of coarse clustering, k-means clustering was conducted for renewable energy power supply and fluctuating load, and the number of clustering centers was set as 3 to obtain three typical power

supply and load operation scenarios and their occurrence probability. According to the output size of renewable energy power supply, it can be divided into three scenarios: source peak, source flat and source valley. Load operation scenarios can be divided into three types: load peak, load flat and load valley. By combining them in pairs, nine typical system scenarios and their occurrence probability are obtained, as shown in Table 2.

TABLE 2. Probabilities of typical scenarios.

System scenario	Probability
Scenario 1 (Source peak, Load peak)	0.0100
Scenario 2 (Source peak, Load flat)	0.1600
Scenario 3 (Source peak, Load valley)	0.0800
Scenario 4 (Source flat, Load peak)	0.0116
Scenario 5 (Source flat, Load flat)	0.1856
Scenario 6 (Source flat, Load valley)	0.0928
Scenario 7 (Source valley, Load peak)	0.0184
Scenario 8 (Source valley, Load flat)	0.2944
Scenario 9 (Source valley, Load valley)	0.1472

B. SUPPLY-DEMAND FLEXIBILITY

According to the power supply and load output data of each scenario, the calculation results of power flow at each moment in this scenario are obtained. Then, according to the calculation results of power flow and the output value of power supply and load in each scene, the flexibility index curve of each scene is obtained by using the calculation formula of the flexibility index of supply and demand in each region.

Taking zone 3 as an example, the supply-demand and down-regulation poor flexibility index curves of three system scenarios (scenario 2, 5 and 8) with the highest probability of occurrence were selected to analyze the impact of renewable energy power output on supply-demand flexibility index. As shown in Figure 9.

As can be seen from Figure 9, in scenario 2, the output of the renewable energy power supply in zone 3 is in the peak state and the load is flat, and the output of the renewable energy power supply can fully meet the demand of the load. Therefore, the poor flexibility index of the up-adjustment in scenario 2 is zero and only needs to be down-regulated. In scenario 5 and 8, as the output of renewable energy power gradually decreases to peak level and peak valley, it will be unable to meet the demand of load fluctuation. At this time, it is necessary to adjust the output of controllable units to meet the demand of load, so the poor flexibility index of scenario 5 and 8 increases gradually. The poor flexibility index of escalation in scenario 5 and 8 is less than 1, indicating that the controllable unit output in zone 3 can meet the flexibility requirement of the zone.

However, in scenario 2, the poor flexibility index of zone 3 is greater than 1 at some moments, indicating that adjustment of controllable unit output at these moments cannot meet the requirement of flexibility reduction, so the

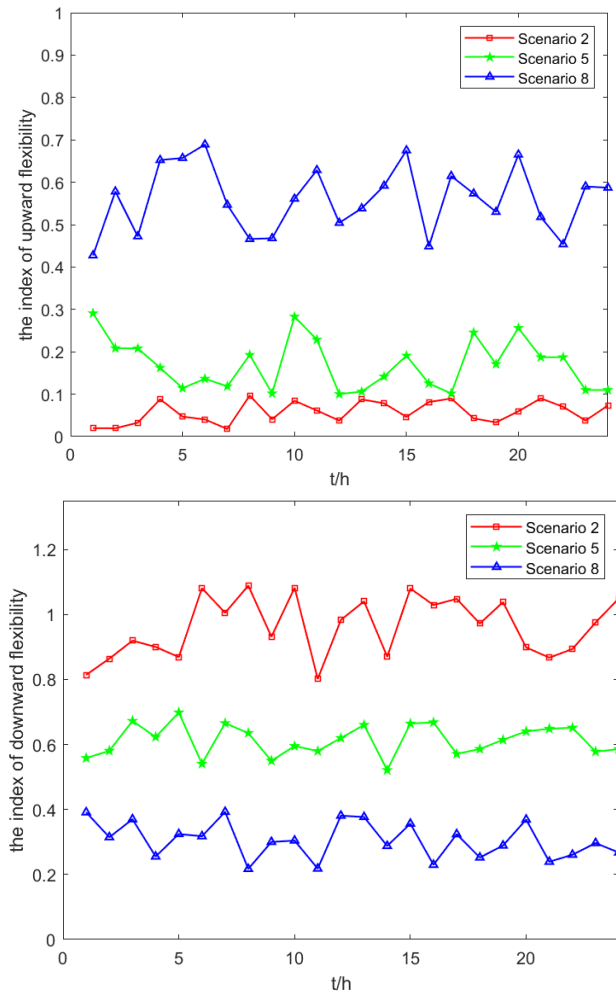


FIGURE 9. System scenario zone 3 supply and demand flexibility indicator.

demand for flexibility reduction can only be met by abandoning renewable energy. In scenario 5 and 8, as the load demand remains unchanged, the renewable energy output gradually decreases and the controllable unit output is not excessively adjusted to meet the load demand, so the poor flexibility index of zone 3 decreases gradually.

Zone 3 was taken as an example to illustrate the influence of renewable energy unit output on the supply and demand flexibility index above, and zone 1 was taken as an example to illustrate the influence of controllable unit output on the supply and demand flexibility index.

In scenario 2, 5 and 8, the poor flexibility index curve of zone 1 as shown in Figure 10.

As can be seen from the figure, in scenarios 2, 5 and 8, the poor flexibility index of supply-demand adjustment in zone 1 increases gradually with the decrease of the output of renewable energy units. The poor flexibility index of the up-regulation at part of scenario 2 is greater than 1, while the poor flexibility index of the up-regulation at each moment of scenario 5 and 8 is greater than 1. This is because the output of the controllable unit in zone 1 is close to the

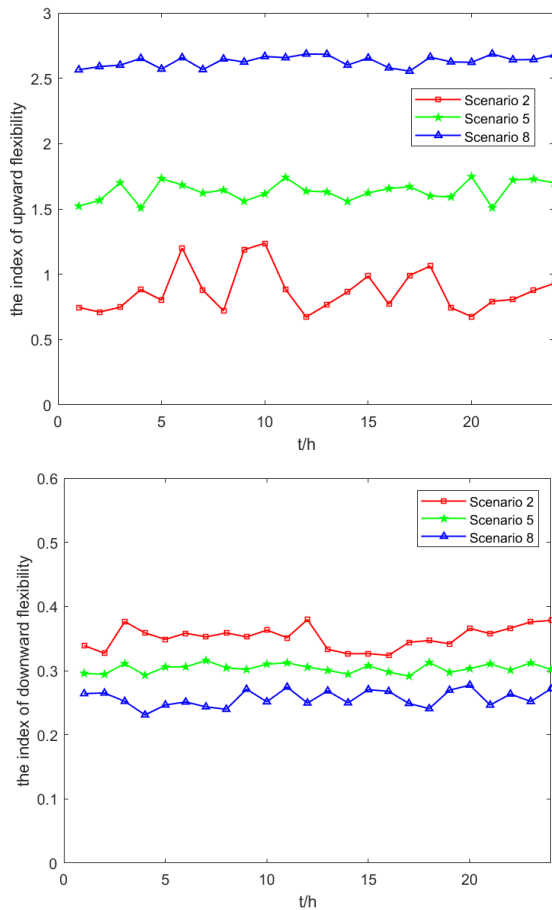


FIGURE 10. System scenario zone 1 supply and demand flexibility indicator.

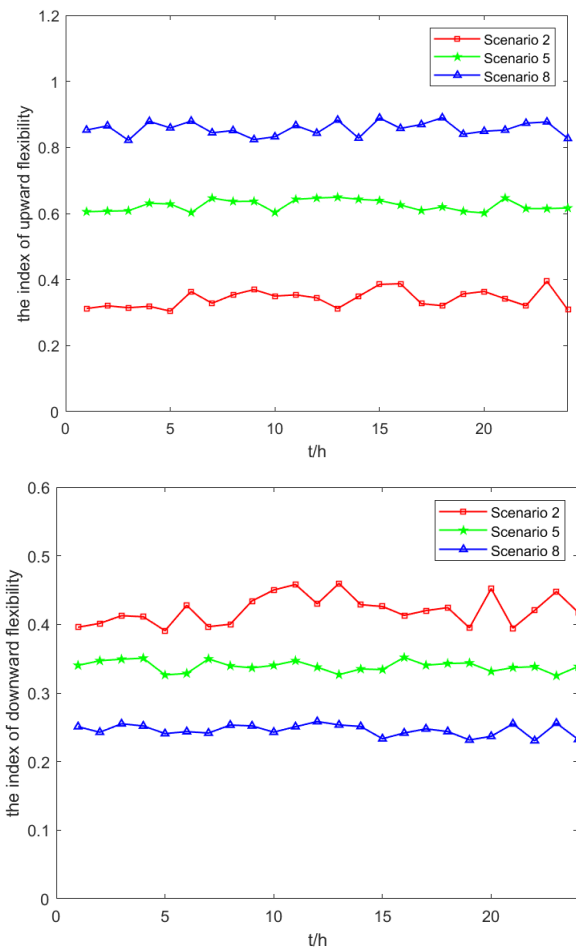


FIGURE 11. Supply and demand flexibility indexes of the whole system.

unit capacity, and the up-regulated capacity is insufficient. The output of renewable energy in scenario 2 is in the peak state, and the output requirement of controllable unit is low. Therefore, the output of controllable unit in Scenario 2 can still meet the load demand at some time. However, the renewable energy output of scenarios 5 and 8 is reduced, and the controllable unit's output cannot meet the flexibility requirement even if it reaches the capacity value. Therefore, the poor flexibility index of scenarios 5 and 8 is greater than 1 at every moment. For zone 1, if the controllable unit has a small room for up-regulation, it means a large room for down-regulation. Therefore, the bad index of down-regulation flexibility of zone 1 in the three scenarios is all less than 1, showing good down-regulation flexibility.

Then, the supply-demand flexibility index of the whole system is analyzed. In scenarios 2, 5 and 8, the poor flexibility index of the whole IEEE39-bus system is lowered on the supply-demand level, as shown in Figure 11.

The figure shows that the whole system on the supply and demand of every moment, poor flexibility index less than 1, that at any time of the whole system control unit output can meet the demand of the flexibility of the whole system supply, however, as stated earlier, some of the entire system

partition, cut flexibility demand cannot meet the problem, Therefore, the flexibility index of supply and demand should be taken into account when the power system is partitioned, and the system should be partitioned reasonably according to the characteristics of controllable units and renewable energy units in different regions.

C. TRANSMISSION CAPACITY FLEXIBILITY

Through the calculation method of transmission capacity flexibility index mentioned above, the poor transmission capacity flexibility index between different zones of the whole system in different typical scenarios after partition can be obtained. Similarly, the three scenarios with the highest probability (scenario 2, 5 and 8) are selected to analyze the inter-regional transmission capacity flexibility index, and the poor transmission capacity flexibility index between different zones in these three scenarios is calculated, as shown in Figure 12.

It can be seen from the figure that in scenarios 2, 5 and 8, the poor flexibility indexes of transmission capacity between each zone are all less than 1, indicating that the transmission capacity of the transmission channel between each zone can meet the requirements of the maximum output

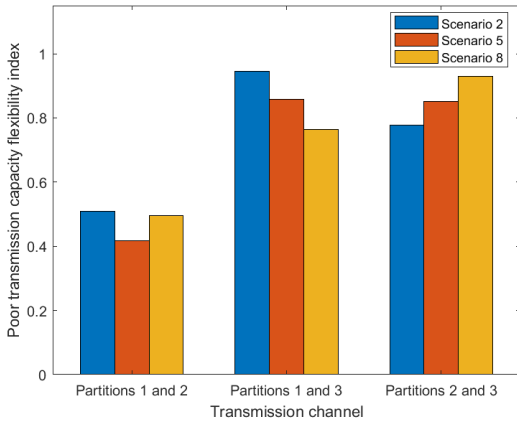


FIGURE 12. Poor flexibility indexes of transmission capacity.

sent by the transmission transmitting end under normal circumstances.

However, sometimes, there will be a fault and exit from the transmission channel of a line, then the transmission capacity between the sending end and the receiving end will be weakened, may be unable to meet the transmission demand, that is, the output of the sending end is blocked. We assume that a transmission line in the transmission channel between each partition breaks down and exits operation, and the resulting poor flexibility index of transmission capacity is shown in Figure 13.

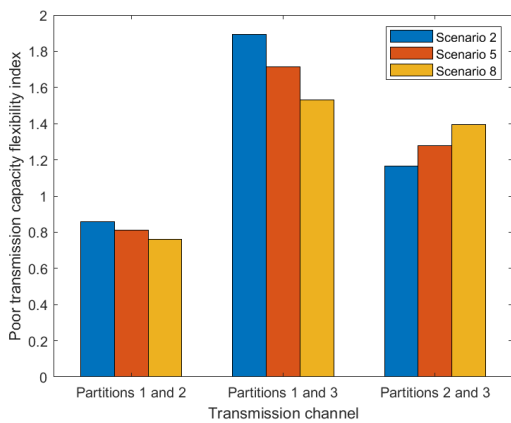


FIGURE 13. Poor flexibility index of transmission capacity under line failure.

In line fault cases, the transmission capacity of poor flexibility index of partitions 1 and 3 and partitions 2 and 3 is greater than 1, shows that when the transmission channels between the partitions of a failure of a transmission line, transmission channel can't meet the demand of transmission, this is where the extension line to improve the transmission capacity of partition between the flexibility. If there is a transport capacity can't meet, will lead to send the output is blocked, making renewable energy sources is deprecated, and if the partition inside force increases with given extra electricity load demand, may influence the distribution of tidal

current, increasing the risk of partition in the transmission line overload, causing the stable operation of the power system.

So, it is necessary to want to consider when to partition the power system partition between the transmission capacity, with the increase of renewable energy units, the sender partition out of electricity, need to make sure that the partition and other partitions between transmission channel transmission capacity to meet the demand of transmission, in order to reduce the sender partition depreciation of renewable energy power supply.

D. OPTIMAL PARTITION RESULT

According to the poor flexibility index of supply-demand and down-regulation of zones in each scenario obtained above, as well as the poor flexibility index of transmission capacity between zones, we think that the weighted coefficients of supply and demand flexibility index, downward flexibility index and transmission capacity flexibility index are the same, then the comprehensive poor flexibility index of power system in each scenario with 3 zones can be calculated, as shown in Table 3. Finally, according to the probability of occurrence of each scenario, the final system comprehensive flexibility index is calculated by weighting. The IEEE39-node system is partitioned for several times, and the number of regions divided is different each time. The comprehensive flexibility index of the system under different partitioning strategies is obtained, as shown in Figure 14.

TABLE 3. Comprehensive poor flexibility index.

Typical scenarios	K_{com}
Scenario 2 (Source peak, Load flat)	0.4932
Scenario 5 (Source flat, Load flat)	0.5531
Scenario 8 (Source valley, Load flat)	0.6156

It can be seen that the composite poor flexibility index of the system in scenario 2 is small, indicating that the system as a whole has good flexibility when the renewable energy output is large.

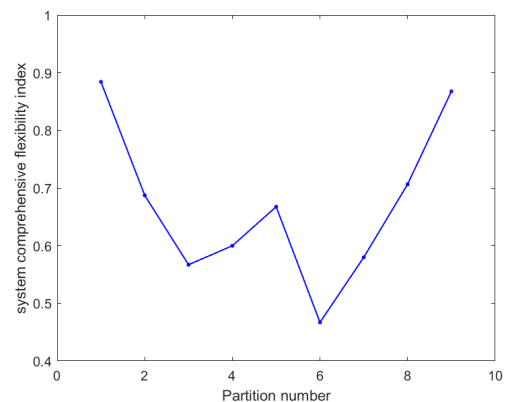


FIGURE 14. System comprehensive flexibility index under different number of partitions.

Figure 14 shows the relationship between the index of poor comprehensive flexibility of the system and the number of partitions. It can be seen that when the number of partitions is 6, the comprehensive flexibility of the system is the best.

The comparison of voltage and loss of IEEE-39 bus nodes under different partitioning strategies is shown in Table 4. It can be seen from Table 4 that the voltage deviation and losses of the system are optimal when the number of partitions is 6.

TABLE 4. Voltage deviation and losses of the IEEE-39 bus bar node.

Partition number	System voltage deviation/%	System losses/MW
1	2.74	55.98
2	2.82	50.24
3	2.70	48.01
4	2.71	47.87
5	2.71	47.12
6	2.65	47.16
7	2.68	48.46
8	2.71	48.57
9	2.79	49.13

Considering the electricity consumption in different time periods, and the electricity price in each time period is shown in Table 5.

TABLE 5. Electricity price for each period.

Electricity consumption	Period of time	Electricity price (\$/kwh ⁻¹)
Peak	10:00-15:00,18:00-21:00	1.059
Flat	7:00-10:00,15:00-18:00,21:00-23:00	0.625
Valley	23:00-0:00,0:00-7:00	0.312

The wind and light abandonment cost is 50 \$/MW, and the load cutting cost is 80 \$/MW. Finally, CPLEX in YALMIP toolbox is called in MATLAB to solve the total cost. The cost of each partitioning scheme is shown in Table 6.

TABLE 6. Cost of each partitioning scheme.

Partition number	Total cost/ (\$)
1	33405
2	32447
3	32316
4	33372
5	31799
6	30530
7	32058
8	32925
9	33663

When the number of zones is 6, the wind abandon rate and light abandon rate of the system are lower because the system

has the lowest comprehensive flexibility index. What's more, due to the higher flexibility of the system, frequent excision load is not required, so the cost of excision load is low. Therefore, the partition scheme with 6 partitions has the lowest total cost.

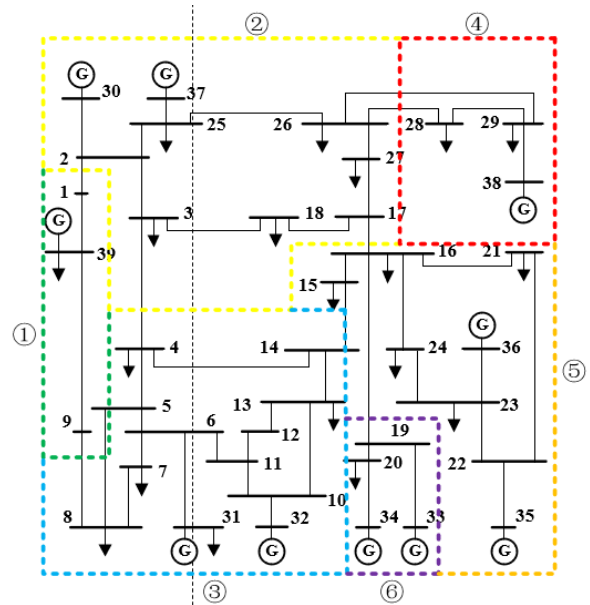


FIGURE 15. Optimal partition result of IEEE 39-bus system.

As shown in Figure 15, the IEEE-39 Bus bar node system is divided into six regions. The system has the lowest comprehensive flexibility index, the supply and demand within the system regions are more easily balanced, and the power transmission between regions will not exceed the rated capacity. In addition, it can be seen from Table 3 that when the output of the renewable energy distribution power supply in the power system is maximum, the power system can operate more safely and stably. For some power systems with fewer nodes, when these power systems need to be partitioned, this method can effectively analyze the quality of the partitioning strategy and determine the final partitioning result.

V. CONCLUSION

In this paper, a dynamic adaptive partitioning method of power grid considering renewable energy and fluctuating load uncertainty is studied based on comprehensive flexibility index of power system. First, a cluster analysis is conducted on the operation scenario of renewable energy and fluctuating load. A large number of historical data of renewable energy and load output are clustered into several operation scenario combinations by improving the K-means clustering algorithm, and the three operating scenario combinations with the highest probability are selected. Then, the poor flexibility index of intra-regional supply and demand balance and the poor flexibility index of inter-regional transmission capacity are proposed, and the comprehensive poor flexibility index is obtained by weighting, so as to evaluate the comprehensive

flexibility of the power system after partitioning. Finally, taking IEEE-39 Bus bar node system as an example, the comprehensive flexibility of each partition scheme is evaluated. It is calculated that when the number of partitions is 6, the system's comprehensive flexibility is the lowest, and the partitioning effect of the scheme is the best. For some power systems with fewer nodes, when these power systems need to be partitioned, this method can effectively analyze the quality of the partitioning strategy and determine the final partitioning result.

The method proposed in this paper still has some defects. When the grid scale is large, the power system partitioning strategy obtained by this method may not be effective. The method in this paper still needs further research. In the future research, the proposed method should overcome the problems of low calculation efficiency of the poor flexibility index and inaccurate evaluation of the comprehensive flexibility index caused by the large number of nodes in the power system.

REFERENCES

- [1] S. N. Azzah, S. Din, M. Ilyas, I. Ashraf, and G. S. Choi, "Resolving energy consumption issues and spectrum allocation for future broadband networks," *IEEE Access*, vol. 9, pp. 166071–166080, 2021.
- [2] Y. Gu, Y. Huang, Q. Wu, C. Li, H. Zhao, and Y. Zhan, "Isolation and protection of the motor-generator pair system for fault ride-through of renewable energy generation systems," *IEEE Access*, vol. 8, pp. 13251–13258, 2020.
- [3] C. Okpalike, F. O. Okeke, E. C. Ezema, P. I. Oforji, and A. E. Igwe, "Effects of renovation on ventilation and energy saving in residential building," *Civil Eng. J.*, vol. 7, pp. 124–134, May 2022.
- [4] S. Singh, "Environmental energy harvesting techniques to power standalone IoT-equipped sensor and its application in 5G communication," *Emerg. Sci. J.*, vol. 4, pp. 116–126, Nov. 2021.
- [5] D. Qerimi, C. Dimitrieska, S. Vasilevska, and A. A. Rrecaj, "Modeling of the solar thermal energy use in urban areas," *Civil Eng. J.*, vol. 6, no. 7, pp. 1349–1367, Jul. 2020.
- [6] S. Nath and S. Rana, "Network reconfiguration for electrical loss minimization," *Int. J. Instrum. Control Autom.*, vol. 1, no. 2, pp. 127–133, Jul. 2011.
- [7] E. Du, N. Zhang, C. Kang, and Q. Xia, "A high-efficiency network-constrained clustered unit commitment model for power system planning studies," *IEEE Trans. Power Syst.*, vol. 34, no. 4, pp. 2498–2508, Jul. 2019.
- [8] B. An, Y. Li, W.-J. Lee, H. Zhou, and F. Zhou, "A multiattribute and multidimensional based comprehensive evaluation method for new multiplex integrated metro traction power supply system," *IEEE Trans. Ind. Appl.*, vol. 56, no. 6, pp. 6138–6149, Nov. 2020.
- [9] H. Nosair and F. Bouffard, "Energy-centric flexibility management in power systems," *IEEE Trans. Power Syst.*, vol. 31, no. 6, pp. 5071–5081, Nov. 2016.
- [10] M. R. Tür, "Reliability assessment of distribution power system when considering energy storage configuration technique," *IEEE Access*, vol. 8, pp. 77962–77971, 2020.
- [11] G. Kara, P. Piscicella, A. Tomsgard, and H. Farahmand, "The impact of uncertainty and time structure on optimal flexibility scheduling in active distribution networks," *IEEE Access*, vol. 9, pp. 82966–82978, 2021.
- [12] E. Lannoye, D. Flynn, and M. O'Malley, "Evaluation of power system flexibility," *IEEE Trans. Power Syst.*, vol. 27, no. 2, pp. 922–931, May 2012.
- [13] Z. Lu, H. Li, and Y. Qiao, "Probabilistic flexibility evaluation for power system planning considering its association with renewable power curtailment," *IEEE Trans. Power Syst.*, vol. 33, no. 3, pp. 3285–3295, May 2018.
- [14] J. Li, Y. Fu, Z. Xing, X. Zhang, Z. Zhang, and X. Fan, "Coordination scheduling model of multi-type flexible load for increasing wind power utilization," *IEEE Access*, vol. 7, pp. 105840–105850, 2019.
- [15] Z. Zhang, Z. Chen, Q. Xing, Z. Ji, and X. Huang, "Comprehensive optimal scheduling strategy of multi-element charging station for bounded rational users," *IEEE Access*, vol. 9, pp. 9442–9452, 2021.
- [16] F. Adamek, M. Arnold, and G. Andersson, "On decisive storage parameters for minimizing energy supply costs in multicarrier energy systems," *IEEE Trans. Sustain. Energy*, vol. 5, no. 1, pp. 102–109, Jan. 2014.
- [17] X. Chen, J. Lv, M. B. McElroy, X. Han, C. P. Nielsen, and J. Wen, "Power system capacity expansion under higher penetration of renewables considering flexibility constraints and low carbon policies," *IEEE Trans. Power Syst.*, vol. 33, no. 6, pp. 6240–6253, Nov. 2018.
- [18] X. Zhu, J. Yang, Y. Liu, C. Liu, B. Miao, and L. Chen, "Optimal scheduling method for a regional integrated energy system considering joint virtual energy storage," *IEEE Access*, vol. 7, pp. 138260–138272, 2019.
- [19] X. Yan and R. Li, "Flexible coordination optimization scheduling of active distribution network with smart load," *IEEE Access*, vol. 8, pp. 59145–59157, 2020.
- [20] H. Yang, H. Peng, J. Zhu, and F. Nie, "Co-clustering ensemble based on bilateral K-means algorithm," *IEEE Access*, vol. 8, pp. 51285–51294, 2020.
- [21] Q. Yang, Y. Liu, D. Zhang, and C. Liu, "Improved K-means algorithm to quickly locate optimum initial clustering number K," in *Proc. 30th Chin. Control Conf.*, 2011, pp. 3319–3322.
- [22] Y. Shima, R. A. Kadir, and F. H. Ali, "A novel approach to the optimization of a public bus schedule using K-means and a genetic algorithm," *IEEE Access*, vol. 9, pp. 73365–73376, 2021.
- [23] M. Li, H. Wang, H. Long, J. Xiang, B. Wang, J. Xu, and J. Yang, "Community detection and visualization in complex network by the density-canopy-K-means algorithm and MDS embedding," *IEEE Access*, vol. 7, pp. 120616–120625, 2019.
- [24] H. Wu, J. Zhang, C. Luo, and B. Xu, "Equivalent modeling of photovoltaic power station based on canopy-FCM clustering algorithm," *IEEE Access*, vol. 7, pp. 102911–102920, 2019.
- [25] X. Tang, Y. Hu, Z. Chen, and G. You, "Flexibility evaluation method of power systems with high proportion renewable energy based on typical operation scenarios," *Electronics*, vol. 9, no. 4, p. 627, Apr. 2020.

GANG YAO is currently a Senior Engineer with the Power Dispatch Control Center of Guizhou Power Grid. His current research interest includes power system dispatching operation and control.

YOUQIAN ZHANG is currently an Assistant Engineer with the Power Dispatch Control Center of Guizhou Power Grid. His current research interest includes power system dispatching operation and control.

TAO ZHANG is currently a Senior Engineer with the Power Dispatch Control Center of Guizhou Power Grid. His current research interest includes power system dispatching operation and control.

QINFENG MA is currently a Senior Engineer with the Power Dispatch Control Center of Guizhou Power Grid. His current research interest includes power system dispatching operation and control.

JINLONG CHEN is currently an Engineer with the Power Dispatch Control Center of Guizhou Power Grid. His current research interest includes power system dispatching operation and control.

• • •